The Cryosphere Discuss., doi:10.5194/tc-2016-52, 2016
Manuscript under review for journal The Cryosphere
Published: 1 April 2016

The Cryosphere Discussions
Open Access
EGU

Basal sliding of temperate basal ice on a rough, hard bed: pressure melting, creep mechanisms and implications for ice streaming

Maarten Krabbendam

British Geological Survey, Lyell Centre, Research Avenue South, Edinburgh EH14 4AP, UK

Correspondence to: Maarten Krabbendam (mkrab@bgs.ac.uk)

Abstract

Basal ice motion is crucial to ice dynamics of ice sheets. The Weertman sliding model for basal sliding over bedrock obstacles proposes that sliding velocity is controlled by pressure melting and/or ductile flow, whichever is the fastest; it further assumes that stoss-side melting is limited by heat flow through the obstacle and ductile flow is controlled by Power Law Creep. These last two assumptions, it is argued here, are invalid if a substantial basal layer of temperate ($T \sim T_{melt}$) ice is present. In that case, frictional melting results in excess basal meltwater and efficient water flow, leading to near-thermal equilibrium. Stoss-side melting is controlled by melt water production, heat advection by flowing meltwater to the next obstacle, and heat conduction through ice/rock over half the obstacle height. No heat flow through the obstacle is required. High temperature ice creep experiments have shown a sharp weakening of a factor 5-10 close to T_{melt}, implying breakdown of Power Law Creep and probably caused by a deformation-mechanism switch to grain boundary pressure melting. Ice streaming over a rough, hard bed, as likely in the Northeast Greenland Ice Stream, may be explained by enhanced basal motion in a thick temperate ice layer.

1 Introduction

The manner in which ice deforms within an ice sheet and moves over its base are critical to accurately model the dynamic past, present and future behaviour of such ice bodies (e.g., Marshall, 2005). The internal deformation of cold ice is fairly well understood, and predictions made on the basis of physical laws (e.g., Glen's flow law) are broadly confirmed by observations (e.g., Dahl-Jensen and Gundestrup, 1987; Patterson, 1994; Ryser et al., 2014;, but see Paterson (1991) for problems with dusty ice, and Hooke (1981) for a general critique). This is not the case for basal sliding, for which many parameters are poorly constrained. Instead, many models of modern ice sheets use an empirical drag factor, derived from observed ice velocity and estimated shear stresses (e.g., MacAyeal et al., 1995; Gudmundsson and Raymond, 2008; Ryser et al., 2014). Using an empirical drag factor is reasonable to describe near-steady state situations, but cannot reliably predict ice

The Cryosphere Discuss., doi:10.5194/tc-2016-52, 2016
Manuscript under review for journal The Cryosphere
Published: 1 April 2016

velocities if parameters such as ice thickness, driving forces and meltwater production change significantly. Ice velocities in ice sheets can vary over several orders of magnitude, with the highest ice velocities (>1 km yr^{-1}) in ice streams (e.g., Joughin et al., 2004; 2010); much of this variability is thought to be caused by variations of the constraints on sliding (e.g., Winsborow et al., 2010).

Hard, rough beds are widespread on the beds of the former Pleistocene ice sheets and also likely beneath the present-day Greenland and Antarctic ice sheets (e.g., Kleman et al., 2008; Eyles, 2012; Rippin, 2014; Krabbendam and Bradwell, 2014; Krabbendam et al., 2015). Warm based basal motion over such beds involves frictional sliding over 'flat areas' without roughness (where ice motion is parallel to the bed) as well as motion past bedrock obstacles, which are typically on the 1-100 m scale. Friction on flat areas is largely controlled by basal debris concentration (e.g., Hallet, 1979; Schweizer and Iken, 1992), with debris/bed contacts responsible for most friction, as demonstrated in sub-glacial observations and experiments (Iverson et al., 2003; Cohen et al., 2006; Zoet et al., 2013). The basis of our understanding of motion past bedrock obstacles on a rough bed goes back to Weertman (1957). The essence of Weertman's sliding model is that basal ice movement past an obstacle is controlled either by stoss-side pressure melting around the obstacle or by ductile flow enhanced by stress concentrations near the obstacle, whichever is the fastest. These principles are regarded here as valid. Numerous studies have improved upon the Weertman sliding model, focussing on more realistic geometries of the bedrock obstacles, more sophisticated analyses of the stresses around the obstacles, and models that allow for lee-side cavitation, which was not allowed in the original model (e.g., Kamb, 1970; Nye, 1970, Lliboutry, 1993; Schoof, 2005).

The Weertman sliding model and most of its derivatives, however, apply two further critical assumptions: (1) that stoss-side pressure melting is limited by heat flow *through the obstacle*, and (2) that the rheology of enhanced ductile flow can be described by 'Glen's flow law'. These basic assumptions have rarely been challenged (but see Lliboutry, 1993). A number of observations, mostly published since the original model, pose problems with these assumptions or have an important bearing on the basal thermal regime:

1) There is experimental evidence that ductile flow of temperate ice (ice at the melting temperature) is very fast (Colbeck and Evans, 1973; Duval, 1977; Morgan, 1991). Furthermore, there is widespread evidence of 'very plastic ice' at the base of (former) ice sheets and glaciers, in the shape of highly curved striations (e.g., Chamberlin, 1888) and ice squeezed into narrow bedrock cracks (Anderson et al., 1982; Rea and Whalley, 1994) as observed in air-filled cavities below active glaciers;
2) There is increasing geomorphological evidence for palaeo-ice streaming on rough, hard bedrock-dominated beds without clear topographic steering. These observations have been reported from the former Laurentide ice sheet, the British Ice Sheet, and deglaciated parts of West Greenland (Smith, 1948; Stokes and Clark, 2003; Roberts and Long, 2005; Bradwell et al., 2008; Eyles, 2012; Bradwell, 2013; Eyles and Putkinen, 2014; Krabbendam et al., 2015). In these areas, the deforming-bed models, commonly invoked to explain fast ice motion (e.g., Alley et al.,

The Cryosphere Discuss., doi:10.5194/tc-2016-52, 2016
Manuscript under review for journal The Cryosphere
Published: 1 April 2016

1987; Hindmarsh, 1997; Winsborow et al., 2010) cannot apply because little or no soft-sediment is present. These palaeo-ice stream zones are surrounded by areas also subjected to wet-based ice erosion suggesting intermediate ice velocities (e.g., Bradwell, 2013), consistent with ice velocity analysis and borehole observations from the Greenland Ice Sheet that show significant warm-based sliding (10-100 m yr^{-1}) outside ice-streams (Lüthi et al., 2002; Ryser et al., 2014, Joughin et al., 2010). Thus, fast ice flow appears to be possible on hard, rough beds and cannot be explained by a simple cold/warm thermal boundary (cf. Payne and Dongelmans, 1997). In Greenland, the massive Northeast Greenland ice stream remains difficult to explain, as current explanations invoke geologically unreasonably high geothermal heat flows (e.g., Fahnenstock et al., 2001).

3) In-situ measurements at a glacier base and experiments have shown that wet-based basal sliding occurs under significant friction, caused by basal-debris / bedrock contacts (Iverson et al., 2003; Cohen et al., 2006; Zoet et al., 2013), generating significant frictional heat at the base;
4) Drilling in Greenland Ice Sheet adjacent to the Jakobshavn Isbrae has documented a basal layer of temperate ice with thickness of c. 30 m (Lüthi et al., 2002), equal or greater than the height of typical bedrock obstacles (roches moutonnées, whalebacks) in most crystalline gneiss terrains (Krabbendam and Bradwell, 2014).
5) Observations on sudden drainage of supraglacial lakes in the ablation zone of the Greenland Ice Sheet have shown that under certain circumstances surface melt water can reach the base of an ice-sheet (e.g., Zwally et al., 2002; Das et al., 2008; Catania et al., 2008; van de Wal et al., 2008). Such water influx will have a significant effect on the basal thermal regime.

A thick temperate layer has thus been observed by drilling (e.g., Lüthi et al., 2002), as well as modelled (e.g., Dahl-Jensen, 1989; Calov and Hutter, 1996; Greve, 1997). The sliding mechanism of temperate ice over a rough, hard bed, however, remains unclear. Below, it will be shown that the two critical assumptions of Weertman sliding (stoss-side melting control by heat flow through an obstacle and enhanced ductile flow controlled by Glen's flow law) are not valid for temperate ice, and alternative controlling mechanisms are proposed. The focus of this paper are the primary thermodynamic and rheological controls, so to achieve an improved conceptual model of basal ice motion around bedrock obstacles, rather than the exact quantification of geometries and stress distributions around such obstacles. The problem of how a temperate layer can grow and be maintained is also discussed. Finally, it is suggested that the development of a temperate basal ice layer may help to explain the occurrence of ice streaming on rough, hard beds, such as seen on deglaciated terrains and possibly relevant to the Northeast Greenland Ice Stream.

2 Weertman's model: the pressure melting component

I first deal with the pressure melting component of the Weertman model. Weertman's model (Weertman, 1957) and potential alternatives are illustrated in a worked example with 800 m ice thickness and ice at the melting temperature at the

The Cryosphere Discuss., doi:10.5194/tc-2016-52, 2016
Manuscript under review for journal The Cryosphere
Published: 1 April 2016

base (h_{ice} = 800 m, P_{ice} ~ 70 bar, and T_m ~ -0.5 °C); with an overall shear stress τ of 124 kPa (Fig. 1a; see Appendix for calculations). In Weertman's model, pressure melting occurs on the stoss side of an obstacle as a result of stress concentration, which is a function of the overall shear stress and the proportion of the surface area of the stoss-side to the spacing between obstacles, given by:

(1) $$\sigma^n_{stoss} = \frac{1}{6}\tau\,\lambda^2(wh)^{-1}$$

where σ^n_{stoss} is the normal stress on the stoss side, acting horizontally; τ is the overall shear stress; λ is the spacing between obstacles; and w and h the width and height of the obstacle, respectively. The stress concentration causes a lowering of the melting temperature ΔT_m on the stoss-side according to:

(2) $$\Delta T_m = -C\sigma^n_{stoss}$$

where C is the pressure melting constant ($7.4 \cdot 10^{-8}$ K Pa^{-1}). In the worked example, with w = 1 m, h = 1 m and τ = 124 kPa (similar to Weertman, 1957) this results in a stoss-side normal stress σ^n_{stoss} = 330 kPa, causing a lowering of the melting point of ΔT_m = -0.025 °C. The stress on the lee-side is lower and the melting temperature is higher by an equal amount. Weertman (1957) envisaged that water freezing on the lee-side released latent heat; this excess heat was seen to be *transported through the obstacle* towards the stoss side where it caused further melting. The resultant heat flux through the obstacle Q_{ob} is then controlled by the total temperature difference between the lee and stoss side ($2\Delta T_m$ = 0.05°C in this example), the thermal conductivity of rock K_r and the length l of the obstacle :

(3) $$Q_{ob} = K_r 2\Delta T_m l^{-1}$$

This heat flux was seen to control the amount of thermal energy available at the stoss side for melting to proceed and hence as controlling the velocity by melting V_{pm} :

(4) $$V_{pm} = H_{ice}\rho_{ice}Q_{ob} = H_{ice}\rho_{ice}K_r 2\Delta T_m l^{-1} \propto l^{-1}$$

where H_{ice} is the heat of fusion of ice ($334 \cdot 10^3$ J kg^{-1}) and ρ_{ice} the density of ice (910 kg m^{-3}). This model has a number of problems. Firstly, if cavitation occurs it is unclear how heat can be transported to the stoss-side (an issue also addressed by Lliboutry, 1993). Secondly, V_{pm} is inversely proportional to the length of the obstacle, following equation (4). This implies that ice flowing around an obstacle that is, say, four times longer than another obstacle (Fig. 1b), would be four times slower, even though this obstacle is more streamlined (having a longer aspect ratio). This result is illogical, contradicts most observed geomorphology (Stokes and Clark, 1999; Bradwell et al., 2008) and is a major weakness of the Weertman model.

3 Basal meltwater production by frictional sliding

Consider sliding over a flat area without obstacles, but over which debris-laden ice slides under friction. Friction produces drag and heat. Frictional heat production Q_{fr} and geothermal heat flow Q_{geo} together control the heat budget at the base of ice sheets. Frictional heat production is controlled by the friction coefficient μ, the normal vertical stress σ_{nv} and the sliding velocity V_{sl} according to:

The Cryosphere Discuss., doi:10.5194/tc-2016-52, 2016
Manuscript under review for journal The Cryosphere
Published: 1 April 2016

(5) $Q_{fr} = \mu\, \sigma_{nv}\, V_{sl} \approx \mu(Pi - Pw)\, V_{sl}$ in [W m^{-2}].

The normal vertical stress σ_{nv} can be taken as the effective pressure, that is ice pressure P_i minus water pressure P_w. A temperate layer of ice has no significant thermal gradient and cannot conduct heat (see Section 4). Any heat produced at the base therefore causes basal melting, with the resultant melting rate M_{rm} (see Appendix) given by:

(6) $M_{rm} = \frac{(Q_{geo}+Q_{fr})}{(H_{ice})}$ in [kg s^{-1} m^{-2}]

The friction coefficient μ, controlled largely by debris concentration, and water pressure P_w are likely to vary significantly in space and time. Iverson et al. (2003) measured μ = 0.05 *in situ* below a glacier; Budd et al. (1979) measured μ = 0.01 - 0.4 for experimental sliding over rocks of different micro-roughness; Zoet et al. (2013) reported μ = 0.01 - 0.05 for experimental sliding at the pressure melting point, but much higher values (μ = 0.2 - 0.6) at colder temperatures and also, intriguingly, for warm-based sliding of ice over sandstone, which suggest that different bedrock lithologies can result in very different friction coefficients and hence basal melting rates.

The potential contribution of frictional heat due to basal sliding is graphically illustrated in Fig. 2, using a range of values for μ and P_w. It is clear that under a range of circumstances, frictional heating can be equal or greater than the geothermal heat flow (see also Patterson, 1994; Calov and Hutter, 1994). Even at μ = 0.05 (close to the friction coefficient of Teflon) heat production can be significant. At moderate sliding velocities (<10 m yr^{-1}), heat production at a warm base can be twice the heat production at a cold base, whilst at high sliding velocities typical of ice streams (>50 m yr^{-1}), frictional heating swamps geothermal heating flow. Uncertain but potentially significant spatial variations in friction coefficient, bed roughness and thickness of temperate ice at the base of an ice sheet further imply that it is not reliable to derive geothermal heat fluxes on the basis of basal melt rates (cf. Fahnestock et al., 2001; Greve, 2005).

The question now becomes: what happens with the water produced by frictional heating? There are two possibilities, not mutually exclusive:

1) The water drains away, initially along a film which may evolve into a dispersed drainage system and further into a channelized drainage system (e.g., Weertman and Birchfield, 1983). Generally water will drain away in the direction of ice flow, ultimately discharge from the ice sheet and thus representing overall mass loss. Any thermal gradient at the base will be continuously smoothed by the advective heat transport of the flowing water. As a result, the whole basal environment (basal ice, water and top of bedrock) is in thermal equilibrium at the pressure melting point.
2) If water cannot drain away freely, the water will remain under pressure. Water may move upwards through the temperate ice layer to the cold-temperate-boundary (CTB), either by percolation or hydraulic fracturing. Here it will refreeze and release its latent heat; this heat will warm up the cold ice just above the CTB, and thus thicken the temperate layer, as further explained below.

The Cryosphere Discuss., doi:10.5194/tc-2016-52, 2016
Manuscript under review for journal The Cryosphere
Published: 1 April 2016

4 Intermezzo: growing and maintaining a temperate ice layer

The growth and continuance of a temperate ice layer below cold ice is an interesting problem in its own right. The problems associated with this are two-fold (Fig. 3):

i) as cold ice above the CTB moves (by internal deformation) towards the margin, there is a strong component of horizontal thermal advection, isotherms are compressed and the thermal gradient at the base of the cold ice just above the CTB is steep, much steeper than can be maintained by heat conduction alone (Patterson, 1994; Dahl-Jensen, 1989; Funk et al., 1994). In Borehole C north of Jakobshavn Isbrae, this thermal gradient has been measured as 0.05 °C m^{-1} (= 50 °C km^{-1}!) (Lüthi et al., 2002). There is thus the tendency to cool and hence shrink the temperate layer. For a temperate layer to exist and grow, energy must thus be added to the CTB (e.g., Clarke et al., 1977; Blatter and Hutter, 1990);

ii) a temperate ice layer has no thermal gradient, so no heat can be conducted through it; it forms an ideal thermal barrier (see also Aschwanden and Blatter, 2005).

Several mechanisms can be invoked to add energy to the CTB, despite there being no thermal gradient (Fig. 3):

1) Bedrock highs can conduct heat: if these penetrate the CTB, heat can be conducted into cold ice. This mechanism is limited by the heat conductivity of rock and the height of the obstacle; it cannot explain a CTB above a bedrock high;

2) Temperate ice layer may locally thicken by internal deformation, i.e. by folding or thrusting for instance where basal ice flow is heterogeneous near obstacles. However, this can only redistribute the CTB, rather than lead to an overall thickening of the temperate layer

3) Strain heating within deforming cold ice above the CTB. Given that this zone is subject to high strain this maybe significant (e.g., Clarke et al., 1977; Iken et al., 1993). However, the sharp nick in the temperature profile in Borehole C (Fig. 3) suggests that most heat is transferred across the CTB, rather than generated within the cold ice above the CTB;

4) Transport of water through the temperate layer. If water moves upward through the temperate layer and crosses the CTB, it freezes, releasing latent heat and warming the cold ice just above the CTB. As the ice temperature rises to T_m, the CTB moves upwards and the temperate layer thickens. A water flux through the temperate layer therefore equates with a heat flow. Temperate ice has a low permeability (Lliboutry, 1971) and such water flow is opposite to gravity but if the subglacial drainage system is poorly connected then locally $P_w > P_i$; (high P_w has been observed in drill hole C in Greenland (Iken et al. 1993)). In that case, water can move upward by hydrauling fracturing. Water may also migrate by capillary action and as bubbles through ductile deformation, as suggested by the experiments of Wilson et al. (1996). Even a small water flux is very effective in transporting 'heat' because of the large latent heat of melting compared to the specific heat capacity of ice: 1 kg of freezing water can heat 160 kg of ice by 1 °C (Paterson, 1994). To maintain the CTB with a thermal gradient of 0.05 °C m^{-1} just above it (e.g., Lüthi et al., 2002), an energy flow of 0.105 W m^{-2} is required, about twice the normal geothermal heat flow (see Appendix). This in turn requires a flux of water through the temperate layer of ~10 mm yr^{-1} (see Appendix), well within the range of water production by frictional melting at

The Cryosphere Discuss., doi:10.5194/tc-2016-52, 2016
Manuscript under review for journal The Cryosphere
Published: 1 April 2016

moderate to high sliding velocities. This latter mechanism is probably the most important to grow and maintain a temperate layer.

5 Stoss-side pressure melting in temperate ice

What are the rate controlling factors for stoss-side pressure melting in a layer of temperate ice? In our conceptual model the temperate layer is thicker than the height of the obstacle. If sufficient water is flowing through the system, heat advection by flowing water will be much more efficient than heat conduction through rock or ice: no significant thermal gradients can build up in such a system and the entire basal system (temperate ice, water, and top rock) is at thermal equilibrium at T_m. The only exception is the stoss-side of a bedrock obstacle, where the melting temperature is continually depressed as a result of the concentrated deviatoric stress acting onto it (Fig. 1c). Thus, the problem of stoss-side pressure melting is reduced to a single 'cold patch' at the stoss side, with a temperature ΔT_{stoss} below the ambient T_m (ΔT_{stoss} = -0.025 °C in the worked example, with similar parameter values as Weertman, 1957). To sustain stoss-side pressure melting, heat needs to be transported only a short distance towards this cold patch: anywhere else is at T_m. Although total ΔT is half compared to the Weertman model (there being no warm patch at the lee side), the transport distance is much smaller. Most obstacles will be wider than high, in which case the critical transport distance is 0.5 h. As a consequence the heat flow towards the stoss side will be greater than in Weertman's model, and it is independent of the length of the obstacle. Cavitation may occur, as this system is not dependent on regelation. The process can work without any regelation in an overall melting environment, which is compatible with the observation of continuous net basal melting at the base of ice sheets (e.g., Fahnestock et al., 2001). If regelation occurs on the lee side (because of lower stress) of one obstacle, any excess heat will be advected by flowing water to the stoss-side of the *ne*xt obstacle. In this process, the rate controlling factors are the height of the obstacle (but not the width or the length) and the efficiency of the heat advection by flowing water. The process is *not* limited by heat flow through the obstacle (cf. Weertman, 1957; Kamb, 1970), and the length of the obstacle becomes irrelevant. This type of stoss-side melting will be faster than in Weertman's model for all but the shortest obstacles, and certainly so for obstacles with $l>h$, which is the case for most observed bedrock bedforms in even the roughest of deglaciated terrains (Bradwell, 2013; Roberts and Long, 2005).

6 Stoss-side pressure melting in temperate ice with surface water input

Influx of surface melt water represent addition of thermal energy and can further aid stoss-side melting and hence basal motion. Consider the dramatic influx of surface melt water by the sudden drainage of supraglacial meltwater lakes in West Greenland (e.g., Das et al., 2008). This water is relatively warm (c. 1° C; Tedesco et al., 2012) and such an influx thus represents a significant addition of thermal energy to the base. Sudden influx of warm melt water may have the following consequences:

The Cryosphere Discuss., doi:10.5194/tc-2016-52, 2016
Manuscript under review for journal The Cryosphere
Published: 1 April 2016

a) Increase of basal water pressure P_w, resulting in a drop in effective pressure P_e, lowering the friction on flat surfaces. Frictional heating and drag on the flats will drop, as long as P_w remains high. Because there is less drag on the flat surfaces, the normal stress σ^n_{stoss} onto the stoss side of obstacles, however, increases (also temporarily), enhancing stoss-side melting and basal melting.

b) The basal system is flushed with water that is well above the ambient T_m. Given the very fast recorded flow of large amounts of water (Das et al., 2008), it is assumed here that little heat is lost during englacial transport. Water entering the basal system at 1 °C is 1.5 °C above T_m and 1.525 °C above the stoss-side melting point. There is thus a steeper thermal gradient between the warm water and the cold stoss-side and more thermal energy is available. This will lead to accelerated stoss-side melting, which continues until all the water temperature has cooled to T_m.

The rate controlling factors of this enhanced stoss-side melting are (i) the flux of surface melt water; (ii) the temperature of this water, (iii) the dissipation of the extra heat, for instance by further melting of ice above the flat surfaces.

In West Greenland, sudden supraglacial meltwater drainage events are accompanied by (a) an immediate (hour time scale) speeding up of surface velocity, with a total horizontal displacement of < 1 m, and vertical uplift of the ice surface on a centimetre scale, followed by (b) a longer period (days) of decelerating but still above-average ice velocity (e.g., Das et al., 2008; Shepherd et al., 2009; Hoffman et al., 2011). The centimetre-scale ice uplift is clearly insufficient to lift basal ice over 1-10 m high obstacles that are likely to exist at the base of the Greenland ice sheet, given its gneiss-dominated bedrock (Roberts and Long, 2005; Krabbendam and Bradwell, 2014). The sudden, short jump is probably due to true sliding as basal ice is pushed higher onto (but not over) sloping obstacles due to an increase of P_w. However, the longer-term (days) increase in ice velocity may well be caused by accelerated stoss-side melting as described above. It is remarkable that the dramatic lake drainage events have a rather muted effect on ice velocity, strongly suggesting that the basal ice in West Greenland is 'stuck' on the stoss sides of pronounced bedrock obstacles. The term 'lubrication' (e.g., Parizek and Alley, 2004; Shannon et al. 2007) is inappropriate to describe the latter process: it is enhanced melting-regelation, rather than a lowering of friction, that leads to the speed-up.

7 Weertman model: the creep component in temperate ice

Weertman (1957) assumed that the creep component of ice flowing around a hard obstacle worked with a rheology according to 'Glen's Flow law', albeit enhanced by stress concentration on the stoss side. This law concerns the general relation between imposed deviatoric stress and resulting strain. The temperature dependence follows the Arrhenius relation, so that the relationship between strain rate $\dot{\varepsilon}$, deviatoric stress σ and temperature is typically described in one dimension as :

(7) $\dot{\varepsilon} = A\sigma^n e^{(-\frac{Q_a}{RT})}$

where A is a constant, R the gas constant, n the stress component and Q_a the activation energy (Glen, 1955; Paterson, 1994; Alley, 1992). This general Power Law is applicable at appropriate conditions to many crystalline materials such as quartz,

The Cryosphere Discuss., doi:10.5194/tc-2016-52, 2016
Manuscript under review for journal The Cryosphere
Published: 1 April 2016

olivine and metals (e.g., Poirier, 1985). For ice, experiments suggest that $n \approx 3$ and $Q_a \approx 80\text{-}120$ kJ mol^{-1} for $T > -10$ °C (e.g., Barnes et al., 1971; Duval et al., 1983; Alley, 1992; Patterson, 1994). Comparisons with borehole tilt deformation studies suggests that this describes the rheology of clean ice reasonably well (e.g., Dahl-Jensen and Gundestrup, 1987; Lüthi et al., 2001). Note that strain rate $\dot{\varepsilon}$ increases exponentially with temperature. The question is whether this Power Law adequately describes the rheology of temperate ice (e.g., Hooke, 1981; Parizek and Alley, 2004) and is thus applicable to temperate ice flow around hard obstacles.

Experimental data compiled by Morgan (1991), all performed under constant stress (1 bar = 10^5 Pa), are plotted in Fig. 3 to illustrate the effect of temperature on the strain rate. The natural logarithmic of strain is plotted against the reciprocal of temperature, so that a straight line would confirm Power Law Creep. For temperatures between -5 and -0.5 °C, the data plot on a straight line, the gradient of which equals ($-Q_a/R$), confirming Power Law Creep over this temperature interval. However, at about -0.02 °C there is a sharp nick in the trend, with strain rates increasing by up to a factor of ten as the melting temperature is approached. These data show that: (i) Power Law Creep (equation 7) does not adequately describe ice creep above -0.2 °C and is invalid for temperate ice (see also Barnes et al., 1971), and (ii) temperate ice is 5-10 times weaker than cold ice just below the nick point (Colbeck and Evans, 1973; Morgan, 1991).

The stress-strain rate dependency for temperate ice is poorly constrained. Experiments at constant temperature (≈ -0.01 °C), but varying stress by Colbeck and Evans (1973) suggest $n = 1.3$; experiments of creep at the melting temperature past a sphere by Byers et al. (2012) also suggest $n < 1.5$; whereas analysis of bulk stress and strain rate of the temperate Glacier de Tsanfleuron suggest $n \approx 1$ (Chandler et al., 2008). It appears that temperate ice shows near-Newtonian viscous behaviour in contrast to the strongly non-Newtonian behaviour ($n \approx 3$) typically assumed for normal Power Law Creep in cold ice. Duval (1977) showed a strong dependency on water content, but this water content likely changes constantly during deformation (Wilson et al. 1996). The rheology of temperate ice is thus utterly different from cold ice, and strongly suggests a switch in deformation mechanism near c. -0.2 °C .

The rate-controlling deformation mechanism of Power Law Creep in ice and other crystalline materials such as quartz and olivine is normally regarded to be intracrystalline creep, mainly by dislocation glide along basal planes (e.g., Duval et al., 1983; Poirier, 1985; Alley, 1992). The dominant deformation mechanism for temperate ice, however, is uncertain. Comparisons with other materials are no help, as water is (almost) unique in that its solid phase is less dense that its liquid phase. Experiments with an indentor pressing into temperate ice led Barnes et al. (1971) to suggest that internal pressure melting was significant (see also Wilson et al. 1996). To distinguish this mechanism from the large-scale stoss-side melting, this mechanism is termed here *grain boundary pressure melting* (GBPS). GBPS works by the principle that grain boundaries orientated at high angles to the maximum deviatoric stress are under higher stress than grain other boundaries (Fig. 4). Pressure melting thus occurs along these grain boundaries, and liquid migrates away (Wilson et al. 1996). Water may refreeze on grain boundaries that are under low stress (e.g., oriented at high angles to the minimum deviatoric stress);

The Cryosphere Discuss., doi:10.5194/tc-2016-52, 2016
Manuscript under review for journal The Cryosphere
Published: 1 April 2016

alternatively, excess water may percolate away through the intragranular network. The net effect is strain. The distance of heat transport to the stressed grain boundaries necessary to sustain GBPS is half the grain size (Fig. 4), some three orders of magnitude smaller than the size of most bedrock obstacles. In their experiments, Barnes et al. (1971) noted the clear presence of liquid on grain boundaries and specifically at triple junctions in support of GBPS; high water content in deforming temperate ice was also seen in experiments by Duval (1977) and Wilson et al. (1996). The process is analogous to pressure solution in soluble rocks such as limestone, in which grain boundaries under high stress are loci for solution, whereas grain boundaries under low stress are loci for precipitation (McClay, 1977; Rutter, 1983). Pressure solution in limestone can be reliably deduced if strain markers such as microfossils are present (McClay, 1977; Ramsay and Huber, 1983); unfortunately, glacial ice does not possess such reliable small-scale strain markers.

Since GBPS works on grain boundaries, it should in principle be a grain-size sensitive mechanism, potentially leading to grain-size reduction (e.g., Zeuch, 1983; de Bresser et al., 2001), whereas Barnes et al. (1971) observed a grain-size increase. Dynamic recrystallization and grain growth, however, is rapid in deforming temperate ice (e.g., Wilson, 1986), thus likely counteracting the grain-size reduction effect. It also likely that dislocation creep, enhanced by the presence of water, continues to operate (Barnes et al., 1971; Wilson et al., 1996). Water along grain boundaries decreases the surface area of grain-to-grain contacts and thus leads to an increase in grain-to-grain contact stresses; this will enhance GBPS as well as dislocation creep (De La Chapelle et al., 1999). A further factor is that any strain heating within the temperate layer will lead to an increase in water content, which is known to further weaken ice (Duval, 1977, Chandler et al., 2008).

A strong crystallographic fabric (strain softening) and concentrations of dust or silt particles are known to significantly weaken cold ice in simple shear (e.g., Lile, 1978; Paterson, 1984, 1991; Dahl-Jensen and Gundestrup, 1987; Azuma, 1994), but whether this leads to further weakening of temperate ice is not known. There is still much unknown about creep in temperate ice; all that can be said is that temperate ice is significantly weaker than, and behaves very differently from, cold ice.

8 Discussion

8.1 Summary of rate-controlling mechanisms

In summary, ice flow around a bedrock obstacle in temperate ice is constrained either by stoss-side pressure melting or by enhanced creep. If a temperate layer exists that is thicker than the height of bedrock obstacles, it is proposed here that stoss-side pressure melting is constrained by:

- Stress concentration on the stoss-side, which depends on the surface area of the stoss-side with respect to the spacing of obstacles, and also to the slope of the obstacles, something not considered here;
- Height of the obstacle, which is critical to the transport distance of heat transport;
- Frictional heating on the flat surfaces, which causes the production of excess meltwater;

The Cryosphere Discuss., doi:10.5194/tc-2016-52, 2016
Manuscript under review for journal The Cryosphere
Published: 1 April 2016

- The efficiency and possible localisation of the local drainage network;
- Input of surface meltwater.

In contrast to the Weertman model, stoss-side pressure melting is *not* constrained by heat flow through the rock obstacle, cavitation is possible, and the length of the obstacle is not relevant.

The enhanced basal creep component of basal motion operates close to or at the melting temperature. The rheology of this deformation is poorly constrained, but does not behave according to standard Power Law Creep, is up to one magnitude faster than Power Law Creep in cold ice, and may involve a significant component of Grain Boundary Pressure Melting. The effects of strain softening and dust particles are uncertain; more laboratory experiments on the deformation of temperate ice may help to better understand creep in temperate ice.

8.2 Basal sliding regimes throughout an ice sheet

The proposed model has implications for ice sheet behaviour and the modelling thereof. Consider a hypothetical half-ice sheet (Fig. 5), based on the thermo-mechanical model by Dahl-Jensen (1989) and with a passing resemblance to the Greenland Ice Sheet. Thermal gradients are strongly affected by horizontal motions as ice velocity exceeds the rate of heat conduction, so that a cold 'tongue' occurs within the ice sheet (e.g., Dahl-Jensen, 1989; Iken et al., 1993). The bed is regarded as rough and hard. Three thermomechanical basal regimes can be distinguished, with a potential fourth operating seasonally.

1) In the cold-based regime, the thermal gradient crosses T_m well into bedrock. All geothermal heat is conducted upwards through the ice. No sliding occurs, and frictional heating is zero. All deformation is internal and can be described by Power Law Creep.

2) At some point the thermal gradient crosses T_m at the base of the ice sheet, and the base is at the pressure melting point. Sliding starts and frictional heating kicks in. In this regime, the friction coefficient will be highly variable as some patches will be frozen, with very high static friction coefficient (Barnes et al., 1971; Budd et al., 1979; Zoet et al., 2013) but low sliding velocities, whereas other patches will be wet, with lower friction coefficient but higher sliding velocities. Excess heat may still be conducted away by the overlying cold ice and water may well regelate onto lee-sides and on overlying ice, thus limiting the amount of water present. In this regime, basal sliding by some form of Weertman sliding is likely. Almost all creep still occurs in cold ice and can be described by Power Law Creep.

3) Continuous frictional heating overwhelms the heat conducting capacity of the overlying ice and a thick temperate layer develops. Where or when this happens depends in part on the thermal structure of the ice sheet, and in particular the thermal gradient near the base: a steeper gradient requires more frictional heating to develop a temperate basal layer. Once a thick temperate ice layer has developed, basal motion occurs according to the processes described above: (i) on the flat surfaces

The Cryosphere Discuss., doi:10.5194/tc-2016-52, 2016
Manuscript under review for journal The Cryosphere
Published: 1 April 2016

frictional sliding occurs; (ii) ductile flow will occur, but much faster than Power Law Creep and including a large component of GBPS; (iii) stoss-side melting will be faster than in Weertman Sliding.

4) if large amounts of surface meltwater can drain to the base of the ice sheet, for instance by periodical drainage of supraglacial lakes, a different temporal thermo-mechanical regime develops. Influx of surface meltwater adds thermal energy to the basal environment; this thermal energy is available in part to further accelerate stoss-side pressure melting.

8.3 Relevance for ice streaming

The corollary of the processes described herein is that if a thick temperate layer is present, basal motion over a hard bed with bedrock humps provides less drag than previously thought. This finding is relevant to ice-sheet modelling. For instance, Peltier et al. (2000) argue that the Laurentide ice Sheet cannot be adequately modelled using a standard 'Glen's flow law' rheology; instead they suggest a different, weaker bulk rheology. This solution, however, is at odds with findings that the bulk rheology of ice in boreholes can be adequately described as Power Law Creep. Instead, it may be more realistic to invoke fast, weak basal motion, even on hard beds, in ice-sheet models. How may this relate to ice-streaming mechanisms? A thick temperate layer has been observed in boreholes adjacent to the Jakobshavn Isbrae and inferred within its centre (Lüthi et al., 2002), whereas boreholes in non-ice streaming parts of the Greenland ice sheet show an absence of a temperate layer (Ryser et al., 2014). Ice streams are widespread and their locations appear to be controlled by a range of factors, of which topographic steering and the presence of soft, deforming sediment bed are seen as the most important (e.g., Winsborrow et al., 2010). There are, however, numerous palaeo-ice streams that neither portray strong topographic channelling, nor have soft-sediment (till) at their base (Bradwell et al., 2008; Bradwell, 2013; Eyles, 2012; Krabbendam et al., 2015).

A modern example of such an ice stream maybe the Northeast Greenland Ice Stream (NEGIS) (Joughin et al., 2001; Fahnestock et al., 2001). While there is topographic steering near its outlet glaciers, topographic steering is weak over much of its length (Joughin et al., 2001). The bedrock geology of Greenland is dominated by Precambrian gneisses, and such rocks almost certainly underlie most of the inland track of the NEGIS. Deglaciated areas of Precambrian gneisses in Canada, Scotland, Scandinavia and Greenland generally show a lack of till, extensively exposed bedrock and a rough landscape of rock knolls and rock basins (Roberts and Long, 2005; Krabbendam and Bradwell, 2014). The occurrence of soft, deformable till below the NEGIS is thus unlikely (cf. Joughin et al., 2001). Using high-resolution radar profiles to reconstruct an isochron stratigraphy, Fahnestock et al. (2001) reported large areas of 'missing' basal ice below the NEGIS, and attributed this to very high, long-term basal melt rates (up to c. 100 mm yr^{-1}). These high basal melt rates were thought to be caused by anomalously high (10 times above normal values) geothermal heat flow. The geophysical evidence for such anomalously high geothermal flow, however, is non-unique and localised, and does not cover the track of the NEGIS; moreover, the contribution of frictional heating to high basal melting rates was not taken into account by Fahnestock et al. (2001). Instead,

I suggest here that much of the NEGIS possesses a thick basal layer of temperate ice, formed and maintained largely by frictional heating. Basal melting rates of 100 mm yr^{-1} are possible in areas of high friction and/or high ice velocity (Fig. 2). In the inversion technique employed by Joughin et al. (2001), a weak basal temperate ice layer would potentially give a similarly low basal drag as a soft, deformable bed.

The existence and distribution of a temperate basal layer below cold ice is potentially an important factor controlling ice dynamics and ice streaming. The occurrence of a basal temperate layer can be detected remotely by using radio-echo sounding at certain frequencies (Björnsson et al., 1996; Murray et al., 2000). The development of a temperate basal layer is in part dependent on the thermal structure of the ice sheet. Future challenges to improve dynamic ice sheet modelling include a better knowledge of the rheology of temperate ice, basal friction and frictional heating, basal roughness and distribution and thickness of the basal temperate layer.

9 Conclusions

Basal motion of ice past hard-bed obstacles involves a competition between stoss-side melting and enhanced creep. In a basal layer of temperate ice, stoss-side melting is not controlled by heat flow through the obstacle, but instead by the thickness of the temperate layer, the availability and flux of basal meltwater and the height of the obstacle. Basal creep in temperate ice is up to ten times faster than dislocation creep by Glen's flow law, suggesting a switch in deformation mechanism. A possible dominant deformation mechanism for creep at the melting temperature is grain boundary pressure melting, aided by fast dynamic recrystallisation and enhanced dislocation creep. Together, this suggest that basal sliding in temperate ice over a rough, hard bed provides less drag and is faster than previously thought; allowing the possibility of fast ice flow over hard, rough beds. Three different thermo-mechanical regimes control basal sliding: (i) cold-based regime, (ii) warm-based but with a thin temperate layer and (iii) warm-based with a substantial temperate layer. The onset zones of (palaeo)ice streams may coincide with a minimum thickness of the temperate layer, and a thick basal temperate ice layer can explain (palaeo)ice streaming over rough, hard beds, possibly including the Northeast Greenland Ice Stream.

Acknowledgements

Doug Macayeal, Martyn Drury and Roderick van der Wal are thanked for encouraging discussions. Sam Roberson is thanked for comments on a previous version of the manuscript. This paper is published with the permission of the Executive Director, British Geological Survey.

The Cryosphere Discuss., doi:10.5194/tc-2016-52, 2016
Manuscript under review for journal The Cryosphere
Published: 1 April 2016

References

Alley, R. B., Blankenship, D. D., Bentley, C. R., and Rooney, S: Till beneath ice stream B: 3. Till deformation: evidence and implications, Journal of Geophysical Research, 95, 8921-29, doi: 10.1029/JB092iB09p08921, 1987.

Alley, R. B.: Flow-law hypotheses for ice-sheet modeling, Journal of Glaciology, 38, 245-56, doi:10.1029/2005JF000320, 1992.

Anderson, R. S., Hallet, B., Walder, J, and Aubry, B. F.: Observations in a cavity beneath Grinnell glacier, Earth Surface Processes and Landforms, 7, 63-70, doi: 10.1002/esp.3290070108, 1982.

Aschwanden, A. and Blatter, H.: Meltwater production due to strain heating in Storglaciären, Sweden, Journal of Geophysical Research, 110, F04024, doi: 10.1029/2005JF000328, 2005.

Azuma, N.: A flow law for anisotropic ice and its application to ice sheets, Earth and Planetary Science Letters, 128, 601-14, doi:10.1016/0012-821X(94)90173-2, 1994.

Barnes, P., Tabor, D., and Walker, J. C. F.: The friction and creep of polycrystalline ice, Proceedings of the Royal Society of London. A. Mathematical and Physical Sciences, 324, 127-55, doi: 10.1098/rspa.1971.0132, 1971.

Björnsson, H., Gjessing, Y., Hamran, S. E., Hagen, J. O., Liestøl, O., Pálsson, F., and Erlingsson, B.: The thermal regime of sub-polar glaciers mapped by multi-frequency radio-echo sounding, Journal of Glaciology, 42, 23-32, 1996.

Blatter, H. and Hutter, K.: Polythermal conditions in Arctic glaciers, Journal of Glaciology, 37, 261-69, 1990.

Bradwell, T., Stoker, M.S., and Krabbendam., M.: Megagrooves and streamlined bedrock in NW Scotland: the role of ice streams in landscape evolution, Geomorphology 97 135-56 doi:10.1016/j.geomorph.2007.02.040, 2008.

Bradwell, T.: Identifying palaeo-ice-stream tributaries on hard beds: Mapping glacial bedforms and erosion zones in NW Scotland, Geomorphology 201, 397-414, doi:10.1016/j.geomorph.2007.02.040, 2013.

Budd, W. F., Keage, P. L., and Blundy, N. A.: Empirical studies of ice sliding, Journal of Glaciology, 23, 157-70, 1979.

Calov, R. and Hutter, K: The thermomechanical response of the Greenland ice sheet to various climate scenarios, Climate Dynamics, 12, 243-60, doi: 10.1007/BF00219499, 1996.

Catania, G. A., Neumann, T. A., and Price, S. F.: Characterizing englacial drainage in the ablation zone of the Greenland ice sheet, Journal of Glaciology, 54, 567-78, doi: 10.3189/002214308786570854 2008.

Chamberlin, T.C.: The rock-scorings of the great ice invasions, US Geological Survey, Annual Report, 7, 155-248, 1888.

Chandler, D., Hubbard, B., Hubbard, A., Murray, T., and Rippin, D.: Optimising ice flow law parameters using borehole deformation measurements and numerical modelling, Geophysical Research Letters, 35, L12502, doi: 10.1029/2008GL033801, 2008.

Clarke, G. K., Nitsan, U., and Paterson, W. S. B.: Strain heating and creep instability in glaciers and ice sheets, Reviews of Geophysics, 15, 235-47, doi: 10.1029/RG015i002p00235, 1977.

Cohen, D., Hooke, R. L., Iverson, N. R., and Kohler, J.: Sliding of ice past an obstacle at Engabreen, Norway, Journal of Glaciology, 46, 599-610, doi: 10.3189/172756500781832747, 2000.

Colbeck, S. C. and Evans, R. J.: A flow law for temperate glacier ice, Journal of Glaciology, 12, 71-86, 1973.

Dahl-Jensen, D. and Gundestrup, N. S.: Constitutive properties of ice at Dye 3, Greenland, in E.D. Waddinton and J Walder (eds.), The Physical Basis of Ice Sheet Modelling, 170: IAHS Publications, 31-43, 1987.

Dahl-Jensen, D.: Steady thermomechanical flow along two-dimensional flow lines in large grounded ice sheets, Journal of Geophysical Research, 94, 10355-62, doi: 10.1029/JB094iB08p10355, 1989.

Das, S. B., Joughin, I., Behn, M. D., Howat, I. M., King, M. A., Lizarralde, D., and Bhatia, M. P: Fracture propagation to the base of the Greenland ice sheet during supraglacial lake drainage., Science, 320 778-81, doi: 10.1126/science.1153360 2008.

De Bresser, J., Ter Heege, J., and Spiers, C.: Grain size reduction by dynamic recrystallization: can it result in major rheological weakening?, International Journal of Earth Sciences, 90, 28-45, doi: 10.1007/s005310000149, 2001.

De La Chapelle, S., Milsch, H., Castelnau, O., and Duval, P.: Compressive creep of ice containing a liquid intergranular phase: Rate-controlling processes in the dislocation creep regime, Geophysical Research Letters, 26, 251-54, doi: 10.1029/1998GL900289, 1999.

Duval, P.: The role of the water content on the creep rate of polycrystalline ice, IAHS Publication, 118, 29-33, 1977.

Duval, P., Ashby, M. F., and Anderman, I.: Rate-controlling processes in the creep of polycrystalline ice, The Journal of Physical Chemistry, 87, 4066-74, doi: 10.1021/j100244a014, 1983.

Eyles, N.: Rock drumlins and megaflutes of the Niagara Escarpment, Ontario, Canada: a hard bed landform assemblage cut by the Saginaw–Huron Ice Stream, Quaternary Science Reviews, 55, 34-49, doi:10.1016/j.quascirev.2012.09.001, 2012.

Eyles, N. and Putkinen, N.: Glacially-megalineated limestone terrain of Anticosti Island, Gulf of St. Lawrence, Canada; onset zone of the Laurentian Channel Ice Stream., Quaternary Science Reviews, 88, 125-34, doi:10.1016/j.quascirev.2014.01.015, 2014.

Fahnestock, M., Abdalati, W., Joughin, I., Brozena, J., and Gogineni, P.: High geothermal heat flow, basal melt, and the origin of rapid ice flow in central Greenland., Science, 297, 2338-42, doi: 10.1126/science.1065370, 2001.

Funk, M, Echelmeyer, K, and Iken, A: Mechanisms of fast flow in Jakobshavns Isbrae, West Greenland: Part II. Modeling of englacial temperatures, Journal of Glaciology, 40, 569585, 1994.

Glen, J. W.: The creep of polycrystalline ice, Proceedings of the Royal Society of London. Series A. Mathematical and Physical Sciences, 228, 519-38, doi: 10.1098/rspa.1955.0066, 1955.

Greve, R.: Application of a polythermal three-dimensional ice sheet model to the Greenland ice sheet: response to steady-state and transient climate scenarios, Journal of Climate, 10, 901-18, 1997.

Greve, R.: Relation of measured basal temperatures and the spatial distribution of the geothermal heat flux for the Greenland ice sheet, Annals of Glaciology, 42, 424-32, doi: 10.3189/172756405781812510, 2005.

Gudmundsson, G. H. and Raymond, M. : On the limit to resolution and information on basal properties obtainable from surface data on ice streams, The Cryosphere, 2, 413-45, doi:10.5194/tc-2-167-2008, 2008.

Hallet, B.: A theoretical model of glacial abrasion, Journal of Glaciology, 23, 39-50, 1979.

Hindmarsh, R.C.A.: Deforming beds: viscous and plastic scales of deformation, Quaternary Science Reviews, 16, 1039-56, doi:10.1016/S0277-3791(97)00035-8, 1997.

Hoffman, M. J., Catania, G. A., Neumann, T. A., Andrews, L. C., and Rumrill, J. A.: Links between acceleration, melting, and supraglacial lake drainage of the western Greenland Ice Sheet Journal of Geophysical Research, 116, F04035, doi: 10.1029/2010JF001934, 2011.

Hooke, R. L.: Flow law for polycrystalline ice in glaciers' comparison of theoretical predictions, laboratory data, and field, Reviews of Geophysics, 19, 664-72, doi: 10.1029/RG019i004p00664, 1981.

Iken, A, Echelmeyer, K, Harrions, W, and Funk, M: Mechanisms of fast flow in Jakobshavns Isbrre, West Greenland: Part I. Measurements of temperature and water level in deep boreholes, Journal of Glaciology, 39, 15-25, 1993.

Iverson, N. R., Cohen, D., Hooyer, T. S., Fischer, U. H., Jackson, M., Moore, P. L., Lappegard, G., and Kohler, J.: Effects of basal debris on glacier flow, Science, 301, 81-84, doi: 10.1126/science.1083086, 2003.

Joughin, I., Fahnestock, M., MacAyeal, D., Bamber, J. L., and Gogineni, P.: Observation and analysis of ice flow in the largest Greenland ice stream, Journal of Geophysical Research, 106, 34021-34, doi: 10.1029/2001JD900087, 2001.

Joughin, I, Abdalati, W, and Fahnestock, M: Large fluctuations in speed on Greenland's Jakobshavn Isbrae glacier, Nature, 432 608-10, doi:10.1038/nature03130, 2004.

Joughin, I., Smith, B. E., Howat, I. M., Scambos, T., and Moon, T. : Greenland flow variability from ice-sheet-wide velocity mapping, Journal of Glaciology, 56, 415-30, doi: 10.3189/002214310792447734, 2010.

Kamb, B: Sliding motion of glaciers: theory and observation, Reviews of Geophysics, 8, 673-728, doi: 10.1029/RG008i004p00673, 1970.

Kleman, J, Stroeven, A P, and Lundqvist, J: Patterns of Quaternary ice sheet erosion and deposition in Fennoscandia and a theoretical framework for explanation Geomorphology, 97 73-90, doi:10.1016/j.geomorph.2007.02.049, 2008.

Krabbendam, M. and Bradwell, T.: Quaternary evolution of glaciated gneiss terrains: pre-glacial weathering vs. glacial erosion, Quaternary Science Reviews, 95, 20-42, doi: 10.1016/j.quascirev.2014.03.013, 2014.

Krabbendam, M, Eyles, N, Putkinen, N, and Bradwell, T: Streamlined hard beds formed by palaeo-ice streams: a review, Sedimentary Geology, doi: 10.1016/j.sedgeo.2015.12.007, 2015.

Lile, R. C.: The effect of anisotropy on the creep of polycrystalline ice, Journal of Glaciology, 21, 475-83, 1978.

Lliboutry, L.: Permeability, brine content and temperature of temperate ice, Journal of Glaciology, 10, 15-29, 1971.

Lliboutry, L.: Internal melting and ice accretion at the bottom of temperate glaciers, Journal of Glaciology, 39, 50-64, 1993.

Lüthi, M, Funk, M, Iken, A, Gogineni, S, and Truffer, M: Mechanisms of fast flow in Jakobshavn Isbrae, West Greenland: Part III. Measurements of ice deformation, temperature and cross-borehole conductivity in boreholes to the bedrock Journal of Glaciology, 48, 369-85, doi: 10.3189/172756502781831322, 2002.

Macayeal, D. R., Bindschadler, R. A., and Scambos, T. A. : Basal friction of ice stream E, West Antarctica, Journal of Glaciology, 41, 247-62, 1995.

Marshall, S. J.: Recent advances in understanding ice sheet dynamics., Earth and Planetary Science Letters, 240 191-204, doi:10.1016/j.epsl.2005.08.016, 2005.

McClay, K.R.: Pressure solution and Coble creep in rocks and minerals; a review, Journal of the Geological Society of London, 134, 57-70, doi: 10.1144/gsjgs.134.1.0057 1977.

Morgan, V. I.: High-temperature ice creep tests, Cold regions science and technology, 19, 295-300, doi:10.1016/0165-232X(91)90044-H 1991.

Murray, T., Stuart, G. W., Miller, P. J., Woodward, J., Smith, A. M., Porter, P. R., and Jiskoot, H. : Glacier surge propagation by thermal evolution at the bed, Journal of Geophysical Research, 105(B6), 13491-507, doi: 10.1029/2000JB900066, 2000.

Nye, J. F.: Glacier sliding without cavitation in a linear viscous approximation., Proceedings of the Royal Society of London, A315, 381-403, doi: 10.1098/rspa.1970.0050 1970.

Parizek, B. R. and Alley, R. B.: Implications of increased Greenland surface melt under global-warming scenarios: ice-sheet simulations, Quaternary Science Reviews, 23, 1013-27, doi:10.1016/j.quascirev.2003.12.024, 2004.

Paterson, W.S.B.: Why ice-age ice is sometimes “soft” Cold Regions Science and Technology, 20, 75-98, doi:10.1016/0165-232X(91)90058-O 1991.

Patterson, W. S. B.: The physics of glaciers, Pergamon, Oxford, 1994.

Payne, A. and Dongelmans, P. W.: Self-organization in the thermomechanical flow of ice sheets, Journal of Geophysical Research, 102, 12219-33, doi: 10.1029/97JB00513, 1997.

Peltier, R.W., Goldsby, D.L., Kohlstedt, D.L., and Tarasov, L: Ice-age ice-sheet rheology: constraints from the Last Glacial Maximum from of the Laurentide ice sheet., Annals of Glaciology, 30 163-76, doi: 10.3189/172756400781820859, 2000.

Poirier, J. P.: Creep of crystals: high-temperature deformation processes in metals, ceramics and minerals, Cambridge University Press, Cambridge, 1985.

Ramsay, J. G. and Huber, M. I.: The Techniques of Modern Structural Geology. Volume 1: Strain Analysis, Academic Press, London, 1983.

Rea, B. R. and Whalley, B. W.: Subglacial observations from Øksfjordjøkelen, north Norway, Earth Surface Processes and Landforms, 19, 659-73, doi: 10.1002/esp.3290190706, 1994.

Rippin, D. M.: Bed roughness beneath the Greenland ice sheet, Journal of Glaciology, 59, 724-32, doi: 10.3189/2013JoG12J212, 2013.

Roberts, D H and Long, A J: Streamlined bedrock terrain and fast ice flow, Jakobshavns Isbrae, West Greenland; implications for ice stream and ice sheet dynamics, Boreas, 34 25-42, doi: 10.1111/j.1502-3885.2005.tb01002.x, 2005.

Rutter, E. H.: Pressure solution in nature, theory and experiment, Journal of the Geological Society of London, 140, 725-40, doi: 10.1144/gsjgs.140.5.0725 1983.

Ryser, C., Lüthi, M. P. , Andrews, L. C., Hoffman, M. J., Catania, G. A., Hawley, R. L., Neumann, T. A., and Kristensen, S. S.: Sustained high basal motion of the Greenland ice sheet revealed by borehole deformation, Journal of Glaciology, 60, 647-60, doi: 10.3189/2014JoG13J196, 2014.

Schoof, C. : The effect of cavitation on glacier sliding., Proceedings of the Royal Society A: Mathematical, Physical and Engineering Science, 461, 609-27, doi: 10.1098/rspa.2004.1350, 2005.

Schweizer, J. and Iken, A.: The role of bed separation and friction in sliding over an undeformable bed, Journal of Glaciology, 38 77-92, 1992.

Shannon, S.R., Payne, A.J., Bartholomew, I.D., van den Broeke, M.R., Edwards, T.L., Fettweis, X., Gagliardini, O., Gillet-Chaulet, F., et al.: Enhanced basal lubrication and the contribution of the Greenland ice sheet to future sea-level rise, Proceedings of the National Academy of Sciences, 110, 14156-61, doi: 10.1073/pnas.1212647110, 2013.

Shepherd, A., Hubbard, A., Nienow, P., King, M., McMillan, M., and Joughin, I.: Greenland ice sheet motion coupled with daily melting in late summer, Geophysical Research Letters, 36, L015001, doi: 10.1029/2008GL035758, 2009.

Smith, H. T. U.: Giant glacial grooves in northwest Canada, American Journal of Science, 246, 503-14, doi: 10.2475/ajs.246.8.503 1948.

Stokes, C. R. and Clark, C. D.: Geomorphological criteria for identifying Pleistocene ice streams Annals of Glaciology, 28 67-74, doi: 10.3189/172756499781821625, 1999.

Stokes, C. R. and Clark, C. D.: Laurentide ice streaming on the Canadian Shield: A conflict with the soft-bedded ice stream paradigm?, Geology, 31, 347-50, doi: 10.1130/0091-7613(2003)031<0347:LISOTC>2.0.CO;2 2003.

Tedesco, M., Lüthje, M., Steffen, K., Steiner, N., Fettweis, X., Willis, I., Bayou, N., and Banwell, A. : Measurement and modeling of ablation of the bottom of supraglacial lakes in western Greenland, Geophysical Research Letters, 39, doi: 10.1029/2011GL049882, 2012.

Van de Wal, R. S. W., Boot, W., Van den Broeke, M. R., Smeets, C. J. P. P., Reijmer, C. H., Donker, J. J. A., and Oerlemans, J.: Large and rapid melt-induced velocity changes in the ablation zone of the Greenland ice sheet., Science, 321 111-13, doi: 10.1126/science.1158540, 2008.

Weertman, J.: On the sliding of glaciers, Journal of Glaciology, 3, 33-38, 1957.

Weertman, J.: Creep deformation of ice, Annual Review of Earth and Planetary Sciences, 11, 215-40, doi: 10.1146/annurev.ea.11.050183.001243, 1983.

Weertman, J. and Birchfield, G. E.: Stability of sheet water flow under a glacier, Journal of Glaciology, 29, 374-82, 1983.

Wilson, C. J. L.: Deformation induced recrystallization of ice: the application of in situ experiments, in S.M. Schmid and M. Casey (eds.), Mineral and Rock Deformation: Laboratory Studies: The Paterson Volume: American Geophysical Union, 213-32., 1986.

Wilson, C. J. L., Zhang, Y., and Stüwe, K.: The effects of localized deformation on melting processes in ice, Cold Regions Science and Technology, 24, 177-89, doi:10.1016/0165-232X(95)00024-6, 1996.

Winsborrow, M. C., Clark, C. D., and Stokes, C. R.: What controls the location of ice streams?, Earth-Science Reviews, 103, 45-59, doi:10.1016/j.earscirev.2010.07.003, 2010.

Zeuch, D.H.: On the inter-relationship between grain size sensitive creep and dynamic recrystallization of olivine, Tectonophysics, 93, 151-68, doi:10.1016/0040-1951(83)90237-8 1983.

Zoet, L. K., Carpenter, B., Scuderi, M., Alley, R. B., Anandakrishnan, S., Marone, C., and Jackson, M.: The effects of entrained debris on the basal sliding stability of a glacier, Journal of Geophysical Research, 118, 656-66, doi:10.1002/jgrf.20052, 2013.

Zwally, H. J., Abdalati, W., Herring, T., Larson, K., Saba, J., and Steffen, K.: Surface melt-induced acceleration of Greenland ice-sheet flow., Science, 297 218-22, doi: 10.1126/science.1072708, 2002.

The Cryosphere Discuss., doi:10.5194/tc-2016-52, 2016
Manuscript under review for journal The Cryosphere
Published: 1 April 2016

Figures

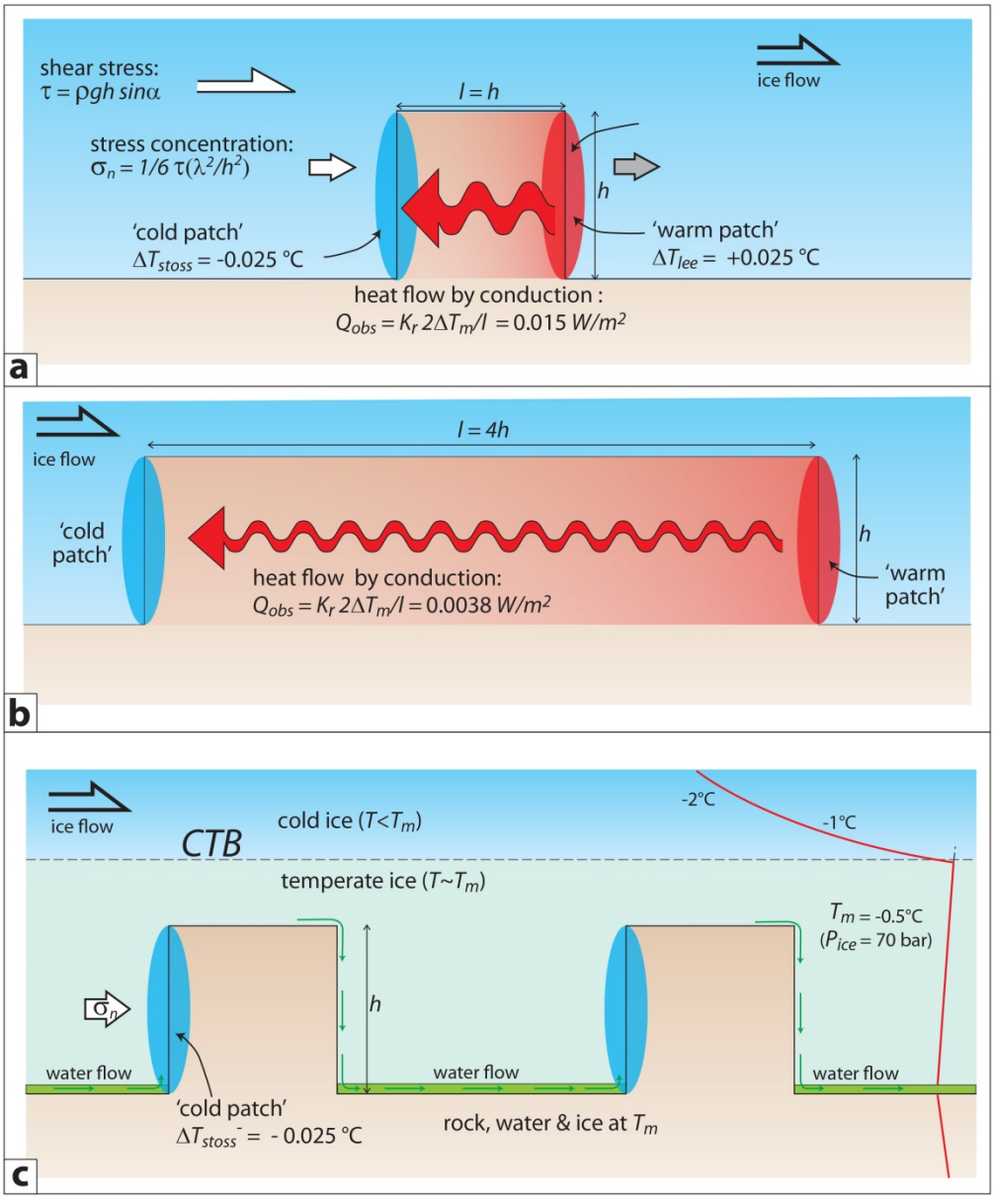

Figure 1. (a) Basic Weertman sliding model, illustrating components of pressure melting. Thermal gradient through bedrock obstacle indicated by gradient grey-scale: darker grey is warmer; (b) Weertman sliding pressure melting with an elongate obstacle, all other parameters are the same; (c) Pressure melting, water and heat transport in a temperate basal layer with significant meltwater flow: a thermal equilibrium occurs everywhere by heat advection by flowing water except at the 'cold patch' of the stoss side. CTB = cold-temperate ice boundary. Schematic thermal gradient of Borehole C is indicated (after Lüthi et al., 2000).

The Cryosphere Discuss., doi:10.5194/tc-2016-52, 2016
Manuscript under review for journal The Cryosphere
Published: 1 April 2016

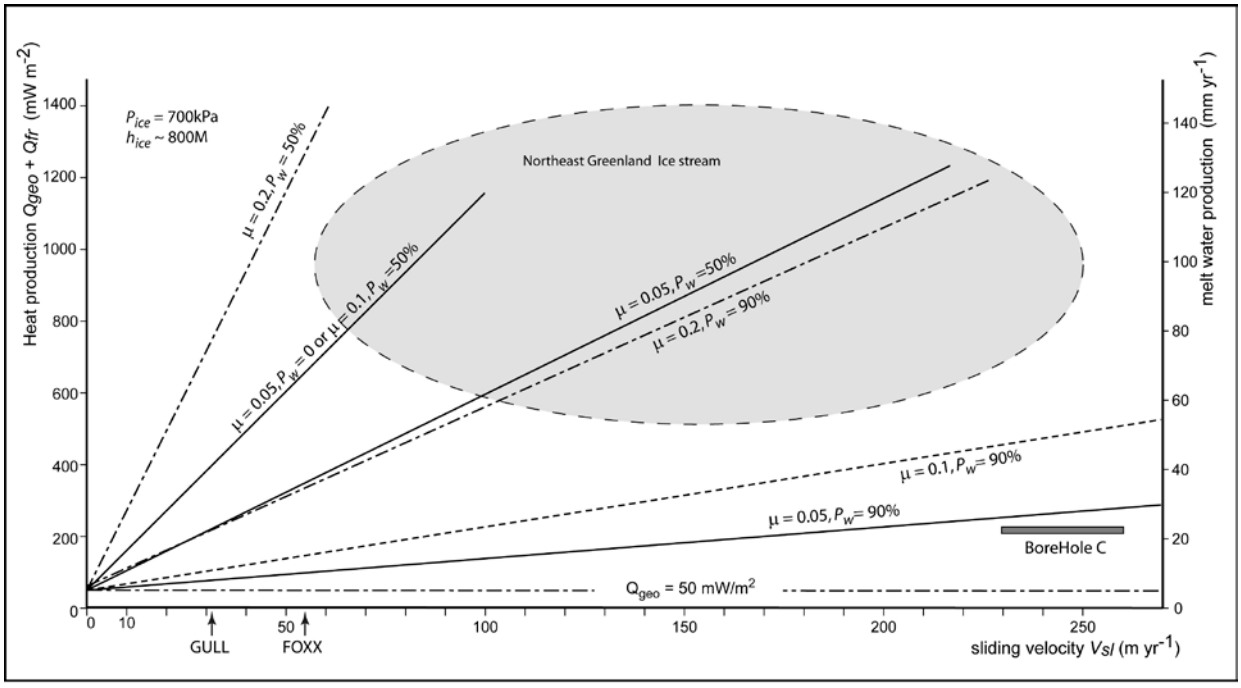

Figure 2. Basal heat production (left) caused by geothermal heat flux and frictional heating as a function of basal sliding velocity, for different values of friction coefficient μ and water pressure P_w as a percentage of overburden pressure. On the right hand side the rate of melt water production, assuming all heat is taken up by melting. Sliding velocities of Borehole C (adjacent to Jakobshavn Isbrae) after Lüthi et al. (2002); melt rate calculated on basis of thermal gradient – see text. Northeast Greenland Ice stream parameters after Joughin et al. (2001) and Fahnestock et al. (2001). GULL, and FOXX are basal sliding velocities deduced from borehole data near Swiss Camp, West Greenland (Ryser et al. 2014).

The Cryosphere Discuss., doi:10.5194/tc-2016-52, 2016
Manuscript under review for journal The Cryosphere
Published: 1 April 2016

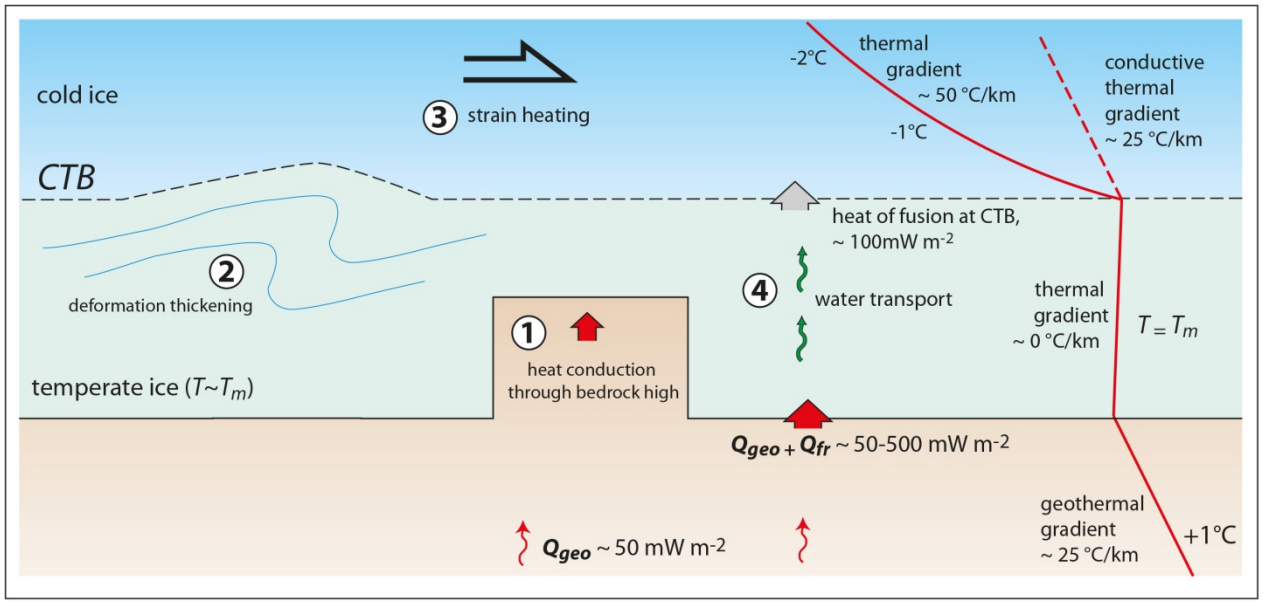

Figure 3. Constraints on the thermal growth of the temperate layer, see text. Schematic thermal gradient of Borehole C is indicated (after Lüthi et al., 2000) . CTB = cold-temperate boundary).

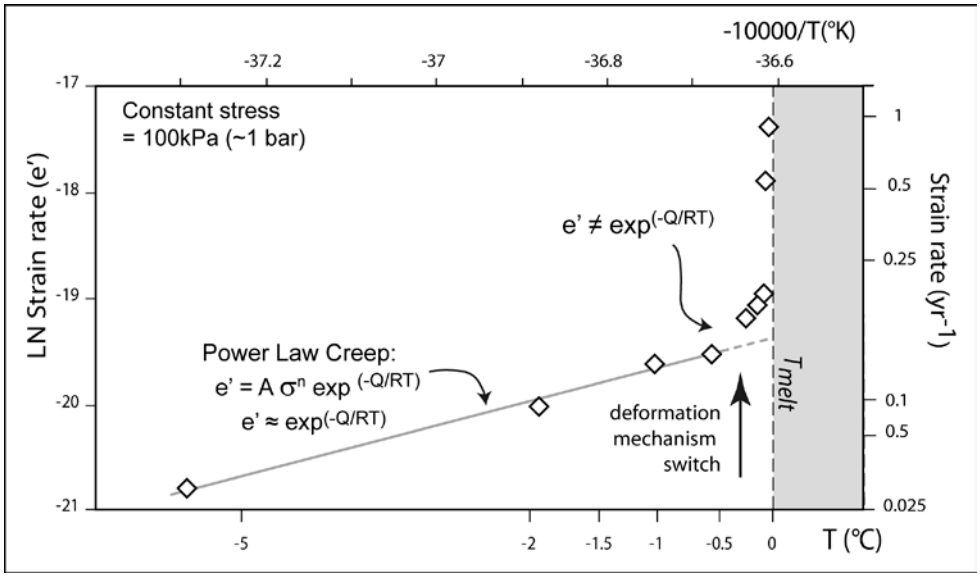

Figure 4. Strain rate against temperature, for experiments performed at 100 kPa, replotted after Morgan (1991). X-axis: reciprocal of temperature; Y-axis: natural logarithm of strain rate, so that data points following Power Law Creep should appear on a straight line.

The Cryosphere Discuss., doi:10.5194/tc-2016-52, 2016
Manuscript under review for journal The Cryosphere
Published: 1 April 2016

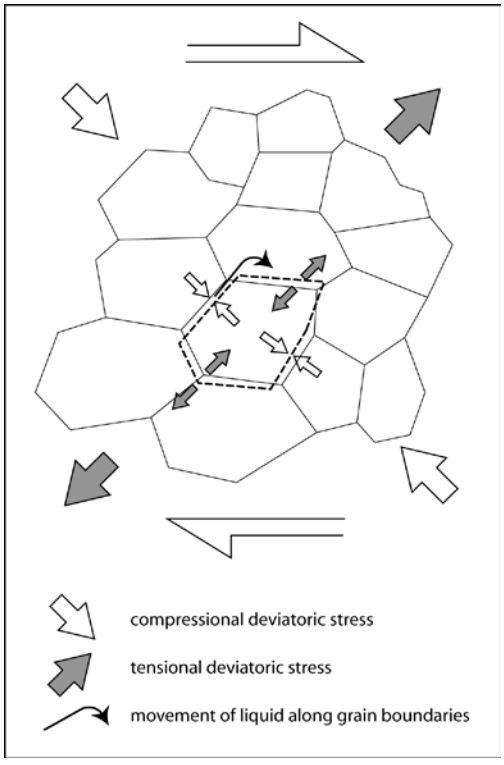

Figure 5. Schematic illustration of grain boundary pressure melting under simple shear. Melting occurs at grain contacts under high stress (compressional deviatoric stress); regelation may occur at grain contacts under low stress (tensional deviatoric stress). Liquid water moves along grain boundaries.

The Cryosphere Discuss., doi:10.5194/tc-2016-52, 2016
Manuscript under review for journal The Cryosphere
Published: 1 April 2016

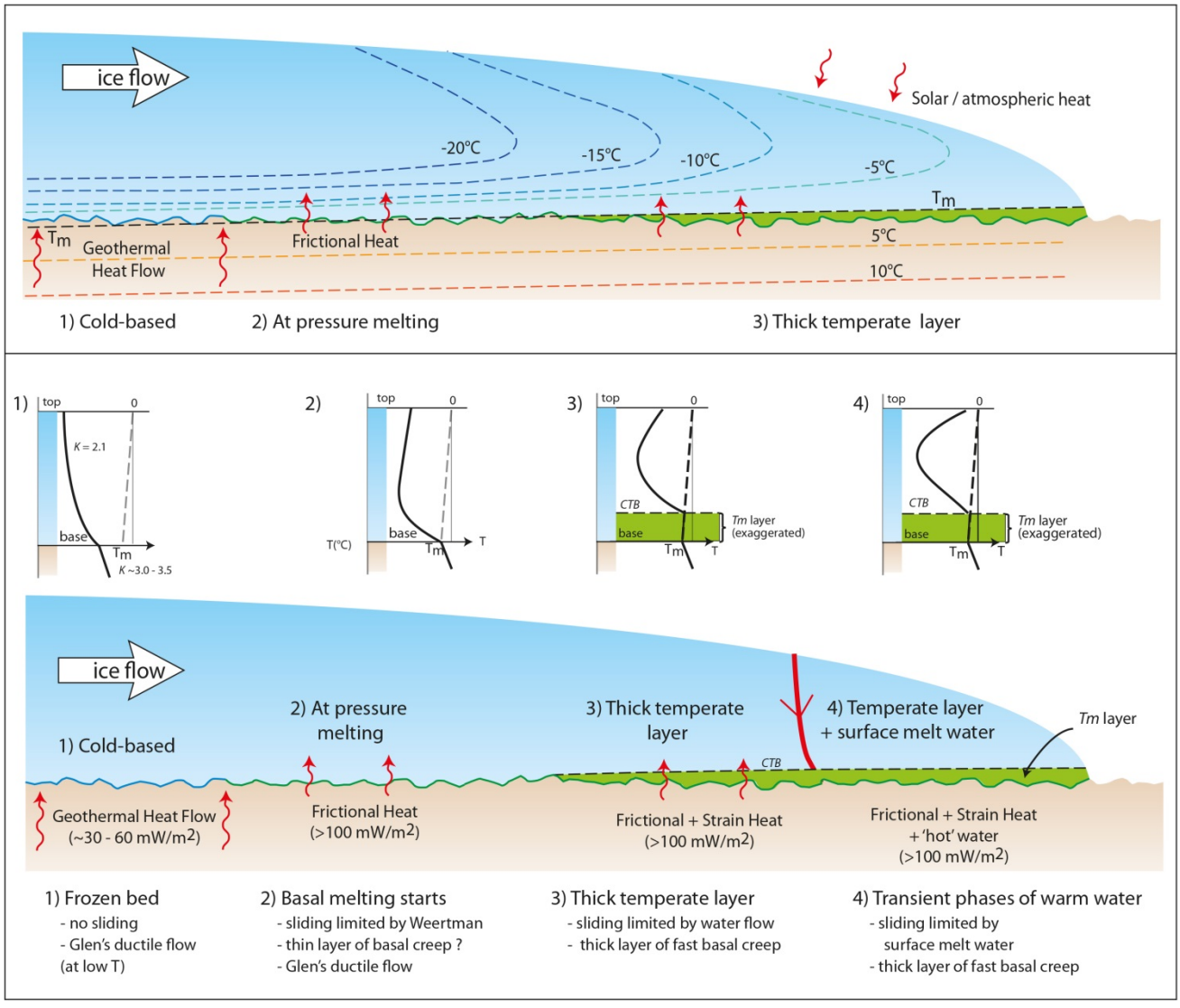

Figure 6. Hypothetical half-ice-sheet (e.g., Dahl-Jensen 1989), with different thermal regimes, further explained in the text. *CTB* = cold-temperate boundary; K = thermal conductivity, T_m = melting temperature. Numbers correspond to different thermal regimes,.

The Cryosphere Discuss., doi:10.5194/tc-2016-52, 2016
Manuscript under review for journal The Cryosphere
Published: 1 April 2016

Table 1

Constant	***Symbol***	**Value**
Density Ice	ρ_{ice}	910 kg m^{-3}
Gravitational constant	G	9.8 m s^{-2}
Thermal conductivity ice	K_{ice}	2.10 $Wm^{-1}K^{-1}$
Thermal conductivity rock	K_r	3.0 $Wm^{-1}K^{-1}$
Heat of fusion ice	H_{ice}	$334 \cdot 10^3$ J kg^{-1}
Year	yr	$3.15 \cdot 10^7$ s
Pressure-melting constant	C	$7.4 \cdot 10^{-8}$ K Pa^{-1}
Gas constant	R	8.314 J K^{-1} mol^{-1}

Variable	***Symbol***	**Unit**
Overall shear stress near base	τ	Pa
Normal stress on stoss side (horizontal)	σ^n_{stoss}	Pa
Normal stress on base (vertical)	σ^n_v	Pa
Heat flow through obstacle	Q_{ob}	W m^{-2}
Heat production by frictional heating (per surface area)	Q_{fr}	W m^{-2}
Melt rate (by mass)	M_r	kg s^{-1} m^{-2}
Melt rate (by volume)	M_r	mm yr^{-1}
Pure sliding velocity	V_{sl}	m s^{-1} or m yr^{-1}
Velocity component by pressure melting	V_{pm}	m s^{-1} or m yr^{-1}
Velocity component by enhanced creep	V_{cr}	m s^{-1} or m yr^{-1}
Water flow across CTB	F_w	kg s^{-1} m^{-2}

Parameter	***Symbol***	**Value**
Ice thickness	h_{ice}	800 m
Surface slope	α	1°
Height obstacle [(1)]	h	1 m
Width obstacle [(1)]	w	1 m
Spacing obstacles [(1)]	λ	4m
Geothermal heat flow [(2)]	Q_{geo}	0.05 W m^{-2}

[(1)] same as Weertman (1957)

[(2)] typical range: 0.03 – 0.07 W m^{-2} = 30 - 70 mW m^{-2}

Table 1. Constants, variables and parameters with chosen values.

The Cryosphere Discuss., doi:10.5194/tc-2016-52, 2016
Manuscript under review for journal The Cryosphere
Published: 1 April 2016

Appendix

Pressure melting temperature is given by:

(A1) $\Delta T_m = -C\Delta P$

The overall pressure is:

(A2) $P_{ice} = \rho_{ice} g h$

With h_{ice} = 800 m, it follows that P_{ice} = 7.13· 10^6 Pa, so that ΔT_m = -0.52 °C.

Shear stress is given by:

(A3) $\tau = \rho g h \sin\alpha$

With surface slope α = 1° and ice thickness h_{ice} = 800 m, the shear stress τ = 1.24 · 10^5 Pa or 124 kPa.

The concentration of horizontal normal stress acting onto a vertical stoss side is given by Weertman (1957):

(A4) $\sigma_{stoss} = \frac{1}{6}\tau\left(\frac{\lambda^2}{wh}\right)$ in [Pa]

Using the same parameters as Weertman (1957): h = 1m, w = 1 m, λ = 4 m and the overall shear stress from equation (A3), τ = 1.24 · 10^5 Pa, it follows that: σ_{stoss} = 3.3 ·10^5 Pa or 330 kPa.

The pressure melting point at the stoss side is given by:

(A5) $\Delta T_{stoss} = -C\sigma^n_{stoss}$ in [°C]

Taking the value of σ^n_{stoss} from Eq. (A4) it follows that: ΔT_{stoss} = -0.024 °C. This is the pressure melting point depression below ambient T_m; so that the T_{stoss} = - 0.544 °C.

Heat flow through obstacle is given by Weertman (1957):

(A6) $Q_{ob} = K_r 2\Delta T_m / l$ in [W m^{-2}]

For an obstacle 1 m long, and taking the value of ΔT_{stoss} from (A5), Q_{ob} = 0.15 W m^{-2}. For an obstacle 4 m long, but with all other parameters the same, the heat flow becomes: Q_{ob} = 0.038 W m^{-2}

Frictional heating is in general given by:

(A7a) $Q_{fr} = \mu\, \sigma_{nv}\, V_{sl}$ in [W m^{-2}]

At the base of an ice sheet this can be expressed as:

(A7b) $Q_{fr} = \mu(Pi - Pw)\, V_{sl}$ in [W m^{-2}]

Assuming all heat is taken up by melting ice, the melt rate is given by:

(A8) $M_{rm} = \frac{(Q_{geo}+Q_{fr})}{(H_{ice})}$ in [kg s^{-1} m^{-2}]

Recalculated in mm yr^{-1}, the melt rate becomes :

The Cryosphere Discuss., doi:10.5194/tc-2016-52, 2016
Manuscript under review for journal The Cryosphere
Published: 1 April 2016

(A9) $M_{rv} = \frac{1000}{\rho_{ice}} * 3.15\ 10^{7}\ \frac{(Q_{geo}+Q_{fr})}{(H_{ice})}$ in [mm yr^{-1}]

To maintain a temperate layer below cold ice with a steep thermal gradient requires a heat flow through the cold-temperate boundary (CTB) of:

(A10) $Q_{CTB} = K_{ice}(dT/dz)$ in [W m^{-2}]

where K_{ice} is the thermal conductivity of ice and dT/dz the thermal gradient just above the CTB. In the case of borehole C near Jakoshavn Isbrae, the thermal gradient is 0.05 °C m^{-1} (Lüthi et al., 2002), requiring Q_{CTB} becomes 2.1 * 0.05 = 0.105 W m^{-2}, about twice the normal geothermal heat flow (compare with Fig. 3).

The transport of energy by water flow through the temperate layer Q_{LAT} that freezes above the CTB is given by:

(A11) $Q_{LAT} = F_w H_{ice}$ in [W m^{-2}]

where F_w is the mass flux of water across the CTB (in kg m^{-2} s^{-1}), and H_{ice} the heat of fusion of ice. A temperate layer will maintain its thickness if $Q_{LAT} = Q_{CTB}$, and will thicken if $Q_{LAT} > Q_{CTB}$. The required mass flux of water thus becomes:

(A12) $F_w = K_{ice}(dT/dz)/\ H_{ice}$ in [kg m^{-2} s^{-1}]

In the worked example of Borehole C, the required mass flux $F_w = 6.6 \cdot 10^{-7}$ kg m^{-2} s^{-1}.

Expressed as a melt rate, using equation A9 (in mm yr^{-1}), M_{rv} = 23 mm yr^{-1}.